

Incremental Object Detection with CLIP

Ziyue Huang, Yupeng He, Qingjie Liu, *Member, IEEE*, and Yunhong Wang, *Fellow, IEEE*

Abstract—In contrast to the incremental classification task, the incremental detection task is characterized by the presence of data ambiguity, as an image may have differently labeled bounding boxes across multiple continuous learning stages. This phenomenon often impairs the model’s ability to effectively learn new classes. However, existing research has paid less attention to the forward compatibility of the model, which limits its suitability for incremental learning. To overcome this obstacle, we propose leveraging a visual-language model such as CLIP to generate text feature embeddings for different class sets, which enhances the feature space globally. We then employ super-classes to replace the unavailable novel classes in the early learning stage to simulate the incremental scenario. Finally, we utilize the CLIP image encoder to accurately identify potential objects. We incorporate the finely recognized detection boxes as pseudo-annotations into the training process, thereby further improving the detection performance. We evaluate our approach on various incremental learning settings using the PASCAL VOC 2007 dataset, and our approach outperforms state-of-the-art methods, particularly for recognizing the new classes.

Index Terms—Object detection, Incremental learning, Multimodal alignment

I. INTRODUCTION

THE human visual system is inherently incremental as individuals acquire new knowledge through observation and integrate it into their existing visual knowledge system. Despite the brilliant progress in object detection achieved by deep learning, existing object detectors [1], [2], [3], [4], [5] still struggle to adapt well when it comes to incremental learning scenarios [6], [7], [8], [9], [10], [11], [12], [13], [14], primarily due to issues such as catastrophic forgetting [15], [16], [17]. In incremental learning scenarios, object detection tasks may encounter data ambiguity [6], which leads to compatibility issues for the current model with both historical and future data, known as backward compatibility and forward compatibility respectively. Most existing works aim to enhance backward compatibility, enabling models to retain previous knowledge. Data ambiguity arises from the specific requirements of incremental detection tasks. In a given task stage, images contain objects belonging to the current stage class, as well as previously learned and potential novel classes. During training, previously learned and new class samples may be incorrectly treated as negative samples, resulting in compatibility issues. This phenomenon is also observed in open world object detection [18]. For instance, IODML [9] employs meta-learning to mitigate deviation, and ERD [19] utilizes elastic distillation to improve classification and

regression. Despite that these methods effectively consolidate prior knowledge, they fall short in fully addressing forward compatibility [20], thereby limiting the model’s growth and adaptability.

To tackle the challenges posed by data ambiguity and forward compatibility, we propose a method called Incremental Object Detection with CLIP (IODC). We use the zero-shot capability of the visual-language pre-trained model (i.e., CLIP [21]) to capture incoming new classes and design corresponding modules to enable the growable capability of the model. Specifically, our approach involves aligning the detectors with text embedding space, which is more appropriate for new classes (Sec. II-B), identifying potential unknown objects with more super-classes in the early stage (Sec. II-C), and employing category mapping for comprehensive knowledge transfer (Sec. II-D). The results demonstrate that our approach has effectively improved the model’s incremental capability, particularly for learning new classes, surpassing other state-of-the-art methods.

The main contributions of our work are as follows: (1) We introduce text feature alignment to align the text features of CLIP with the region features of the detector, enabling the detector to detect unknown objects. (2) We introduce the concept of super-classes, facilitating fine-grained potential object identification. Additionally, we extend pseudo-annotations using the CLIP image encoder, augmenting the model’s awareness of novel classes. (3) We propose category mapping for effective knowledge transfer to novel classes. (4) Extensive experiments demonstrate that our approach outperforms state-of-the-art methods in the incremental detection task, significantly improving the accuracy of new classes.

II. METHOD

A. Problem Formulation

As illustrated in Fig. 1, incremental learning involves sequential multiple tasks [6], constituting a continuous data flow. Each task T_i introduces a group of classes denoted as C_i , ensuring no overlap with class sets introduced in other tasks, i.e., $C_i \cap C_j = \emptyset (i \neq j)$. The classes in the current task are denoted as C_{base} , while the classes of future tasks are labeled as C_{novel} .

During the T_i stage, the model M_i is trained using only the data from the current class set C_i . The model M_i comprises a feature extractor F , a classification head G , and a regression head for incremental detection. By leveraging the text-to-image alignment feature of CLIP, we enable the detector to recognize potential classes during base training, enhancing the model’s forward prediction capabilities and improving its continuous learning ability.

Ziyue Huang, Yupeng He, Qingjie Liu, and Yunhong Wang are with the State Key Laboratory of Virtual Reality Technology and Systems, Beihang University, Beijing 100191, China, and also with the Hangzhou Innovation Institute, Beihang University, Hangzhou 310051, China (e-mail: ziyuehuang@buaa.edu.cn; heyupeng@buaa.edu.cn; qingjie.liu@buaa.edu.cn; yhwang@buaa.edu.cn).

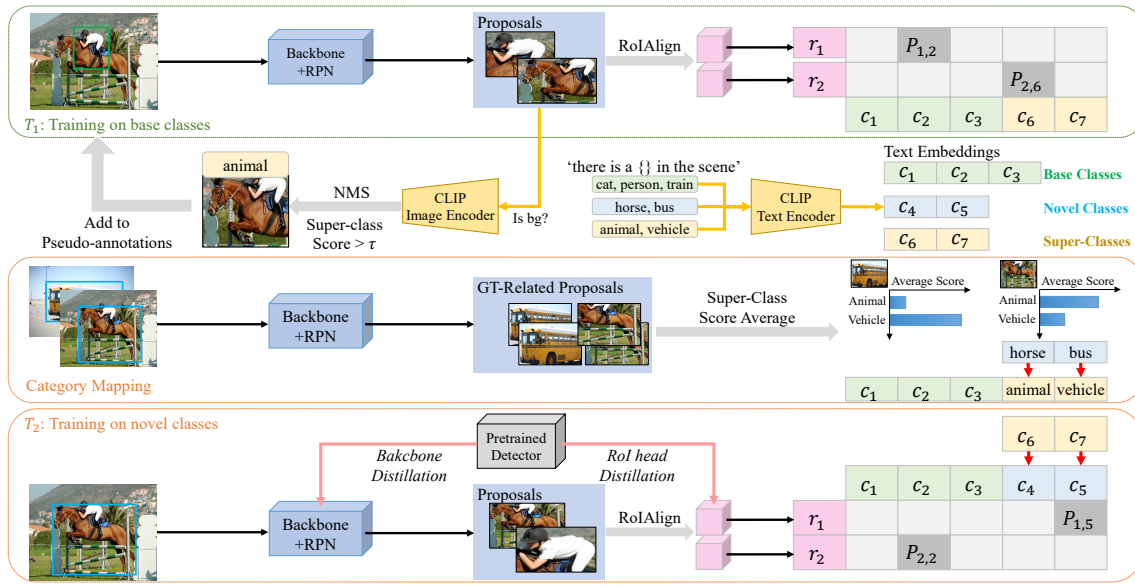


Fig. 1: IODC uses the CLIP text encoder to obtain text embeddings. In the T_1 task, IODC firstly trains the detector with base classes, and utilizes the CLIP image encoder to generate pseudo-annotations for super-classes. Then, the detector is retrained with both base classes and pseudo-annotations. Subsequently, we use category mapping to establish correspondences between novel classes and super-classes. Finally, in the T_2 task, the correspondence is leveraged for training novel classes.

B. Text Feature Alignment

One drawback of the traditional framework [1] is that its classification head G can only predict the category within the closed set. To overcome this limitation, as illustrated in Fig. 1, we modify the classification output layer to a linear mapping layer, obtaining the region visual embeddings $\{r_i\}_{i=1}^{N_r}$, where N_r denotes the number of regions. Subsequently, we construct a prompt template [24], such as ‘there is a *object* in the scene,’ with the *object* representing one of the class names. We then input these prompts containing the class names into the CLIP text encoder to obtain the class text embeddings $\{c_j\}_{j=1}^{N_c}$, where N_c denotes the number of classes. The probability of r_i belonging to c_j is calculated as:

$$P_{i,j} = \frac{\exp(r_i \cdot c_j / \tau)}{\sum_j \exp(r_i \cdot c_j / \tau)} \quad (1)$$

where τ is the temperature, set to 0.1 to make the predicted distribution more precise. The predicted distribution is supervisedly trained using cross-entropy loss. By aligning the predicted visual embeddings with the text embeddings, we enable the model to detect incoming new classes and reserve space in its embeddings for the growth of new classes [20].

C. Identify Potential Objects

Since obtaining the exact names of novel classes C_{novel} is impossible, we introduce the super-classes C_{super} . A super-class is the parent category for specific classes, including animals, furniture, machines, etc. Using the CLIP text encoder with prompts, we generate the text embeddings of the base and super-classes and train the model in T_{base} .

During training, the detector generates a large number of box predictions. We match these predicted boxes with the ground truth of C_{base} . For negative sample boxes that do

not match any ground truth, we crop the image patches corresponding to the boxes and send them into the CLIP image encoder to predict the scores for each super-class. Suppose CLIP recognizes the category as belonging to C_{super} , and its confidence score exceeds a predefined threshold τ . In such cases, we assign the corresponding super-class to the box and train the model using cross-entropy loss to draw attention to the super-classes.

In addition to direct supervision, we retain the detected boxes matched with the corresponding super-classes as pseudo-annotations for subsequent training. To ensure the quality of these pseudo-annotations, we use Non-Maximum Suppression (NMS) to filter the detection boxes. And only detected boxes with confidences greater than τ and sizes larger than 100×100 pixels are retained. This process ultimately yields a repository of high-quality pseudo-annotations for super-classes.

D. Category Mapping for Novel Classes

The semantic differences between super-class and novel class hinder the learning process of novel classes in T_2 . To tackle this challenge, we introduce category mapping to transfer the super-class knowledge learned by the detector in task T_1 to novel classes in task T_2 . Firstly, we freeze the model obtained in task T_1 and simulate training on the data from T_2 . During this process, objects for each novel class are matched with multiple proposals, allowing us to obtain super-class scores corresponding to the proposals. We average all the super-class scores of matched proposals for each novel class, yielding the distribution of super-classes, as illustrated in Fig. 1. The distribution allows us to establish correspondence between the novel and super-class classes. Subsequently, we replace the ground truth novel labels with the corresponding super-class labels and train for several iterations. As a result,

TABLE I: Comparison of per-class AP and mAP for incremental object detection on PASCAL VOC 2007. We consider 10+10, 15+5 and 19+1 settings. There are two tasks total, and the classes introduced in the second task are marked with grey. IODML [9] is the work of incremental detection and the baseline for our comparison. ORE and OW-DETR are the works of open world object detection. Our method achieves the highest detection performance under three settings.

| 10+10 setting | aero | cycle | bird | boat | bottle | bus | car | cat | chair | cow | table | dog | horse | bike | person | plant | sheep | sofa | train | tv | mAP |
|--------------------|------|-------|------|------|--------|------|------|------|-------|------|-------|------|-------|------|--------|-------|-------|------|-------|------|-------------|
| Oracle 20 | 79.4 | 83.3 | 73.2 | 59.4 | 62.6 | 81.7 | 86.6 | 83.0 | 56.4 | 81.6 | 71.9 | 83.0 | 85.4 | 81.5 | 82.7 | 49.4 | 74.4 | 75.1 | 79.6 | 73.6 | 75.2 |
| First 10 | 78.9 | 78.6 | 72.0 | 54.5 | 63.9 | 81.5 | 87.0 | 78.2 | 55.3 | 84.4 | - | - | - | - | - | - | - | - | - | - | 36.7 |
| ILOD [6] | 69.9 | 70.4 | 69.4 | 54.3 | 48.0 | 68.7 | 78.9 | 68.4 | 45.5 | 58.1 | 59.7 | 72.7 | 73.5 | 73.2 | 66.3 | 29.5 | 63.4 | 61.6 | 69.3 | 62.2 | 63.1 |
| Faster ILOD [22] | 72.8 | 75.7 | 71.2 | 60.5 | 61.7 | 70.4 | 83.3 | 76.6 | 53.1 | 72.3 | 36.7 | 70.9 | 66.8 | 67.6 | 66.1 | 24.7 | 63.1 | 48.1 | 57.1 | 43.6 | 62.2 |
| IODML [9] | 76.0 | 74.6 | 67.5 | 55.9 | 57.6 | 75.1 | 85.4 | 77.0 | 43.7 | 70.8 | 60.4 | 66.4 | 76.0 | 72.6 | 74.6 | 39.7 | 64.0 | 60.2 | 68.5 | 60.5 | 66.3 |
| ORE [23] | 63.5 | 70.9 | 58.9 | 42.9 | 34.1 | 76.2 | 80.7 | 76.3 | 34.1 | 66.1 | 56.1 | 70.4 | 80.2 | 72.3 | 81.8 | 42.7 | 71.6 | 68.1 | 77.0 | 67.7 | 64.6 |
| OW-DETR [18] | 61.8 | 69.1 | 67.8 | 45.8 | 47.3 | 78.3 | 78.4 | 78.6 | 36.2 | 71.5 | 57.5 | 75.3 | 76.2 | 77.4 | 79.5 | 40.1 | 66.8 | 66.3 | 75.6 | 64.1 | 65.7 |
| IODC (Ours) | 66.6 | 75.0 | 62.6 | 49.1 | 53.6 | 75.5 | 83.5 | 76.4 | 43.0 | 73.3 | 56.1 | 76.1 | 84.8 | 77.9 | 78.4 | 42.1 | 71.2 | 63.2 | 72.6 | 69.2 | 67.6 |

| 15+5 setting | aero | cycle | bird | boat | bottle | bus | car | cat | chair | cow | table | dog | horse | bike | person | plant | sheep | sofa | train | tv | mAP |
|--------------------|------|-------|------|------|--------|------|------|------|-------|------|-------|------|-------|------|--------|-------|-------|------|-------|------|-------------|
| Oracle 20 | 79.4 | 83.3 | 73.2 | 59.4 | 62.6 | 81.7 | 86.6 | 83.0 | 56.4 | 81.6 | 71.9 | 83.0 | 85.4 | 81.5 | 82.7 | 49.4 | 74.4 | 75.1 | 79.6 | 73.6 | 75.2 |
| First 15 | 78.1 | 82.6 | 74.2 | 61.8 | 63.9 | 80.4 | 87.0 | 81.5 | 57.7 | 80.4 | 73.1 | 80.8 | 85.8 | 81.6 | 83.9 | - | - | - | - | - | 53.2 |
| ILOD [6] | 70.5 | 79.2 | 68.8 | 59.1 | 53.2 | 75.4 | 79.4 | 78.8 | 46.6 | 59.4 | 59.0 | 75.8 | 71.8 | 78.6 | 69.6 | 33.7 | 61.5 | 63.1 | 71.7 | 62.2 | 65.9 |
| Faster ILOD [22] | 66.5 | 78.1 | 71.8 | 54.6 | 61.4 | 68.4 | 82.6 | 82.7 | 52.1 | 74.3 | 63.1 | 78.6 | 80.5 | 78.4 | 80.4 | 36.7 | 61.7 | 59.3 | 67.9 | 59.1 | 67.9 |
| IODML [9] | 78.4 | 79.7 | 66.9 | 54.8 | 56.2 | 77.7 | 84.6 | 79.1 | 47.7 | 75.0 | 61.8 | 74.7 | 81.6 | 77.5 | 80.2 | 37.8 | 58.0 | 54.6 | 73.0 | 56.7 | 67.8 |
| ORE [23] | 75.4 | 81.0 | 67.1 | 51.9 | 55.7 | 77.2 | 85.6 | 81.7 | 46.1 | 76.2 | 55.4 | 76.7 | 86.2 | 78.5 | 82.1 | 32.8 | 63.6 | 54.7 | 77.7 | 64.6 | 68.5 |
| OW-DETR [18] | 77.1 | 76.5 | 69.2 | 51.3 | 61.3 | 79.8 | 84.2 | 81.0 | 49.7 | 79.6 | 58.1 | 79.0 | 83.1 | 67.8 | 85.4 | 33.2 | 65.1 | 62.0 | 73.9 | 65.0 | 69.1 |
| IODC (Ours) | 78.0 | 77.2 | 73.2 | 53.5 | 57.8 | 78.3 | 84.1 | 78.4 | 50.2 | 80.1 | 61.5 | 80.3 | 83.3 | 83.5 | 77.9 | 41.6 | 66.2 | 59.2 | 70.9 | 68.4 | 70.2 |

| 19+1 setting | aero | cycle | bird | boat | bottle | bus | car | cat | chair | cow | table | dog | horse | bike | person | plant | sheep | sofa | train | tv | mAP |
|--------------------|------|-------|------|------|--------|------|------|------|-------|------|-------|------|-------|------|--------|-------|-------|------|-------|------|-------------|
| Oracle 20 | 79.4 | 83.3 | 73.2 | 59.4 | 62.6 | 81.7 | 86.6 | 83.0 | 56.4 | 81.6 | 71.9 | 83.0 | 85.4 | 81.5 | 82.7 | 49.4 | 74.4 | 75.1 | 79.6 | 73.6 | 75.2 |
| First 19 | 76.3 | 77.3 | 68.4 | 55.4 | 59.7 | 81.4 | 85.3 | 80.3 | 47.8 | 78.1 | 65.7 | 77.5 | 83.5 | 76.2 | 77.2 | 46.4 | 71.4 | 65.8 | 76.5 | - | 67.5 |
| ILOD [6] | 69.4 | 79.3 | 69.5 | 57.4 | 45.4 | 78.4 | 79.1 | 80.5 | 45.7 | 76.3 | 64.8 | 77.2 | 80.8 | 77.5 | 70.1 | 42.3 | 67.5 | 64.4 | 76.7 | 62.7 | 68.3 |
| Faster ILOD [22] | 64.2 | 74.7 | 73.2 | 55.5 | 53.7 | 70.8 | 82.9 | 82.6 | 51.6 | 79.7 | 58.7 | 78.8 | 81.8 | 75.3 | 77.4 | 43.1 | 73.8 | 61.7 | 69.8 | 61.1 | 68.6 |
| IODML [9] | 78.8 | 77.5 | 69.4 | 55.0 | 56.0 | 78.4 | 84.2 | 79.2 | 46.6 | 79.0 | 63.2 | 78.5 | 82.7 | 79.1 | 79.9 | 44.1 | 73.2 | 66.3 | 76.4 | 57.6 | 70.2 |
| ORE [23] | 67.3 | 76.8 | 60.0 | 48.4 | 58.8 | 81.1 | 86.5 | 75.8 | 41.5 | 79.6 | 54.6 | 72.8 | 85.9 | 81.7 | 82.4 | 44.8 | 75.8 | 68.2 | 75.7 | 60.1 | 68.9 |
| OW-DETR [18] | 70.5 | 77.2 | 73.8 | 54.0 | 55.6 | 79.0 | 80.8 | 80.6 | 43.2 | 80.4 | 53.5 | 77.5 | 89.5 | 82.0 | 74.7 | 43.3 | 71.9 | 66.6 | 79.4 | 62.0 | 69.8 |
| IODC (Ours) | 78.8 | 78.9 | 73.4 | 59.2 | 58.9 | 75.9 | 85.0 | 83.9 | 51.6 | 83.6 | 65.8 | 82.0 | 84.6 | 78.4 | 78.2 | 48.9 | 75.5 | 67.5 | 73.4 | 62.5 | 72.3 |

the detector can temporarily retain super-class knowledge and adapt to novel class images. Finally, we directly train the detector with the novel ground truth. This two-stage training approach helps stabilize the training process and effectively inherits the detection capabilities of the super-class. Additionally, we utilize knowledge distillation and sampler rehearsal methods, commonly used in incremental learning, to improve the model's performance for old classes.

III. EXPERIMENTS

A. Experimental Settings

We undertake a series of incremental detection experiments to assess the efficacy of our proposed method.

Datasets and Evaluation. According to the ILOD [6], we evaluate our proposed method on the PASCAL VOC 2007 dataset [25]. The dataset comprises 9,963 images of 20 categories, accounting for nearly 24,000 instances. Half of the data is allocated for training and validation, with the remaining portion dedicated to testing. We use the mean average precision at 0.5 IoU threshold (mAP@50) to assess the detection performance. We also pay extra attention to the independent mAP of the model on C_{base} and C_{novel} in different tasks, especially for the accuracy of novel classes.

We implement our code utilizing IODML [9] and adhered to their experimental settings. We alphabetically arrange the 20 category names in PASCAL VOC 2007 and categorize them into three typical incremental experimental settings: 10+10, 15+5, and 19+1. The tasks are delineated as T_1 and T_2 . In the 15+5 setting, the data of the first 15 base classes can be accessed in T_1 , and the data of the remaining 5 novel classes can be accessed in T_2 .

Implementation Details. We construct our detector using Faster-RCNN [1], employing pre-trained ResNet-50 [26] as the backbone. We incorporate the strategies of knowledge distillation and sampler rehearsal from IODML. In the T_2 task, we duplicate the frozen parameter model from T_1 , and perform both backbone distillation and ROI distillation. The experiments are performed using 4 RTX3090s, with a total batch size of 8. We use the SGD optimizer with an initial learning rate of 0.02, gradually reduced to 0.0002, a momentum of 0.9, and a warm-up cycle of 100 iterations.

We utilize CLIP ViT-B/32 [21] to generate text embeddings and detect unknown objects. Our experiments chose ten pre-defined class names, including woodwork, pet, mount, bike, person, plant, animal, furniture, vehicle, and machine. We set a confidence threshold of $tr = 0.7$ to ensure the reliability of pseudo-boxes.

B. Results on VOC

Table I presents the per-class AP50 and mAP in each setting on the VOC dataset. The introduced novel classes are shaded in grey. Our method is evaluated in a scenario with two incremental tasks and is compared with three incremental detection methods (ILOD [6], Faster ILOD [22], and IODML [9]) as well as two open world detection approaches (ORE [23] and OW-DETR [18]). The second row illustrates the Oracle model, portraying the upper bound performance for each class through complete supervised learning on all training images. Our proposed method outperforms the current state-of-the-art in all incremental settings, attaining approximately a +2% improvement for all classes in each setting.

In Table II, we present the mAP results of our proposed method for base classes and novel classes at different stages.

TABLE II: Ablation experiments on PASCAL VOC 2007. The comparison is shown in base classes mAP, novel classes mAP, and overall mAP. The 'text', 'super', and 'pseudo' refer to the text feature alignment, super-class, and pseudo-annotations. For the 15+5 setting, base classes are the first 15 classes, and novel classes are the remaining 5 classes.

| 10+10 setting | | Ablation Studies | | | T_1 | | | T_2 | | |
|---------------|------|------------------|--------|--------------|-------------|--------------|--------------|--------------|--------------|--|
| Methods | text | super | pseudo | base | novel | all | base | novel | all | |
| Oracle 20 | | | | - | - | - | 74.72 | 75.66 | 75.19 | |
| First 10 | | | | 73.40 | 0 | 36.70 | - | - | - | |
| IODML [9] | | | | 75.31 | 0 | 37.65 | 68.36 | 64.26 | 66.31 | |
| ORE [23] | | | | - | - | - | 60.37 | 68.79 | 64.58 | |
| OW-DETR [18] | | | | - | - | - | 63.48 | 67.88 | 65.68 | |
| IODC (Ours) | ✓ | | | 74.91 | 2.83 | 38.87 | 66.49 | 65.37 | 65.93 | |
| | ✓ | ✓ | | 75.26 | 0.36 | 37.81 | 66.81 | 65.60 | 66.21 | |
| | | | ✓ | 75.59 | 6.88 | 41.23 | 66.05 | 65.61 | 65.83 | |
| | ✓ | ✓ | ✓ | 76.95 | 5.36 | 41.16 | 66.06 | 69.15 | 67.61 | |
| 15+5 setting | | Ablation Studies | | | T_1 | | | T_2 | | |
| Methods | text | super | pseudo | base | novel | all | base | novel | all | |
| Oracle 20 | | | | - | - | - | 76.78 | 70.42 | 75.19 | |
| First 15 | | | | 76.85 | 0 | 57.64 | - | - | - | |
| IODML [9] | | | | 69.78 | 0 | 56.26 | 71.73 | 55.90 | 67.77 | |
| ORE [23] | | | | - | - | - | 73.21 | 58.68 | 68.51 | |
| OW-DETR [18] | | | | - | - | - | 72.21 | 59.84 | 69.12 | |
| IODC (Ours) | ✓ | | | 76.30 | 3.56 | 58.12 | 73.11 | 59.20 | 69.63 | |
| | ✓ | ✓ | | 75.61 | 2.73 | 57.39 | 72.21 | 57.99 | 68.66 | |
| | | | ✓ | 76.20 | 6.56 | 58.79 | 72.81 | 60.93 | 69.84 | |
| | ✓ | ✓ | ✓ | 76.73 | 9.21 | 59.85 | 73.14 | 61.23 | 70.16 | |
| 19+1 setting | | Ablation Studies | | | T_1 | | | T_2 | | |
| Methods | text | super | pseudo | base | novel | all | base | novel | all | |
| Oracle 20 | | | | - | - | - | 76.78 | 70.42 | 75.19 | |
| First 19 | | | | 71.07 | 0 | 67.52 | - | - | - | |
| IODML [9] | | | | 73.39 | 0 | 69.72 | 70.89 | 57.60 | 70.23 | |
| ORE [23] | | | | - | - | - | 69.35 | 60.10 | 68.89 | |
| OW-DETR [18] | | | | - | - | - | 70.18 | 62.00 | 69.78 | |
| IODC (Ours) | ✓ | | | 74.42 | 2.18 | 70.81 | 72.27 | 59.92 | 71.65 | |
| | ✓ | ✓ | | 74.42 | 0.54 | 70.73 | 72.12 | 58.21 | 71.43 | |
| | | | ✓ | 73.87 | 5.26 | 70.44 | 72.20 | 62.40 | 71.71 | |
| | ✓ | ✓ | ✓ | 74.27 | 3.64 | 70.74 | 72.82 | 62.45 | 72.30 | |

TABLE III: Effect of adding more redundant super-classes. K is the number of redundant classes added.

| 15+5 setting | | K values | T_1 | | | T_2 | | |
|--------------|----|------------|-------|-------|-------|-------|-------|-------|
| | | | base | novel | all | base | novel | all |
| IODC | - | - | 76.30 | 3.56 | 58.12 | 73.11 | 59.20 | 69.63 |
| IODC | 5 | 76.54 | 1.47 | 57.77 | 72.81 | 60.93 | 69.84 | |
| | 10 | 76.50 | 2.31 | 57.95 | 73.33 | 60.39 | 70.10 | |
| | 15 | 76.28 | 0.84 | 57.42 | 73.38 | 59.78 | 69.98 | |
| | 30 | 76.66 | 1.37 | 57.84 | 73.82 | 58.74 | 70.75 | |
| | 60 | 76.40 | 0.42 | 57.41 | 73.56 | 57.91 | 69.65 | |

We also report the performance upper bound of an Oracle model, a detector trained on ground-truth for all classes. As expected, the Oracle model achieves the highest performance on all class sets (C_{base} , C_{novel} , and C_{all}). ORE and OW-DETR are open world studies, so they cannot provide mAP results in the T_1 stage. Compared to these methods, our approach can distinguish different potential objects in T_1 through super-class matching. This mechanism can further integrate with the category mapping to detect novel classes at T_1 and effectively improve the novel performance at T_2 . At the T_2 stage, our method generally has a higher mAP for novel classes.

C. Ablation Studies

Effect of each module. After aligning text features using explicit base and novel classes, we observe an overall improvement in mAP for both base and novel classes. This suggests that incorporating text features into the visual model

TABLE IV: Effect of confidence threshold τ .

| 15+5 setting | τ values | T_1 | | | T_2 | | |
|--------------|---------------|--------------|-------------|--------------|--------------|--------------|--------------|
| | | base | novel | all | base | novel | all |
| IODML [9] | - | 75.01 | 0 | 56.26 | 71.73 | 55.90 | 67.77 |
| IODC (Ours) | 0.5 | 76.89 | 3.66 | 58.13 | 72.34 | 59.11 | 69.03 |
| | 0.7 | 76.73 | 9.21 | 59.85 | 73.14 | 61.23 | 70.16 |
| | 0.9 | 75.73 | 4.36 | 57.88 | 71.53 | 59.89 | 68.62 |

can be beneficial, and CLIP can extract semantic information from class names. However, after introducing the super-class, we observe a slight decrease in mAP, possibly due to the more ambiguous semantics of super-categories. Since we cannot obtain the precise novel classes, the decrease in performance with the introduction of super-categories is acceptable. On the other hand, the pseudo-annotations significantly enhance the detection ability of the model for novel classes at T_1 by introducing pseudo-bounding boxes identified by the CLIP image encoder. By combining all three methods, we achieved the best results. These results demonstrate the effectiveness of our proposed methods for incremental detection. By improving the model's detection ability for novel classes in the T_1 stage and transferring this knowledge to the T_2 stage, we have made the model more forward compatible and enabled it to achieve a higher mAP of novel classes.

Effect of super-classes. We validate the impact of the number of super-classes on performance. Specifically, we add more categories from COCO [27] under the 15+5 learning setting and evaluate the performance in Table III. As the number of redundant categories K increases, the overall effect of the experiment remains stable. However, when $K \geq 30$, the model's learning ability for novel classes fluctuates. Therefore, we only use a fixed set of ten super-classes to guide the learning of forward perception.

Effect of threshold τ . The confidence threshold τ will affect the quantity and quality of pseudo-annotations. Experiments in Table IV indicate that using a too-high confidence threshold adversely affects the available target boxes, resulting in poor performance. On the other hand, a lower threshold can yield more valid target boxes, but the reliability cannot be guaranteed. However, regardless of the parameter settings, the model significantly improves the novel class at T_2 . After careful consideration, a threshold setting of 0.7 is identified as optimal.

IV. CONCLUSIONS

Due to the challenge of data ambiguity, existing incremental detection methods struggle with learning novel classes. To address this issue and enhance the forward compatibility of the model, we propose the IODC method. Firstly, we align the region features of the detector with the text features generated by CLIP, enabling the detector to detect arbitrary classes. Furthermore, we introduce the concept of a super-class and leverage CLIP's text-to-image feature alignment to detect potential classes. Subsequently, we propose category mapping to facilitate a smooth transition into learning novel classes. Our approach significantly enhances the model's ability to detect novel categories without the need for additional datasets and outperforms the state-of-the-art method on benchmark datasets.

REFERENCES

- [1] S. Ren, K. He, R. Girshick *et al.*, “Faster r-cnn: Towards real-time object detection with region proposal networks,” in *Adv. Neural Inf. Process. Syst.*, vol. 28, 2015.
- [2] J. Redmon, S. Divvala, R. Girshick, and A. Farhadi, “You only look once: Unified, real-time object detection,” in *IEEE Conf. Comput. Vis. Pattern Recognit.*, 2016, pp. 779–788.
- [3] T.-Y. Lin, P. Goyal, R. Girshick, K. He, and P. Dollár, “Focal loss for dense object detection,” in *IEEE Int. Conf. Comput. Vis.*, 2017, pp. 2980–2988.
- [4] S. Chen, Z. Li, and Z. Tang, “Relation r-cnn: A graph based relation-aware network for object detection,” *IEEE Signal Process. Lett.*, vol. 27, pp. 1680–1684, 2020.
- [5] T. Cheng, L. Song, Y. Ge, W. Liu, X. Wang, and Y. Shan, “Yolo-world: Real-time open-vocabulary object detection,” in *IEEE Conf. Comput. Vis. Pattern Recognit.*, 2024.
- [6] K. Shmelkov, C. Schmid, and K. Alahari, “Incremental learning of object detectors without catastrophic forgetting,” in *IEEE Int. Conf. Comput. Vis.*, 2017, pp. 3400–3409.
- [7] J. Perez-Rua, X. Zhu, T. Hospedales *et al.*, “Incremental few-shot object detection,” in *IEEE Conf. Comput. Vis. Pattern Recognit.*, 2020, pp. 13 846–13 855.
- [8] D. Yang, Y. Zhou, A. Zhang *et al.*, “Multi-view correlation distillation for incremental object detection,” *Pattern Recognit.*, vol. 131, p. 108863, 2022.
- [9] K. Joseph, J. Rajasegaran, S. Khan *et al.*, “Incremental object detection via meta-learning,” *TPAMI*, vol. 44, no. 12, pp. 9209–9216, 2021.
- [10] Y. Wu, Y. Chen, L. Wang, Y. Ye, Z. Liu, Y. Guo, and Y. Fu, “Large scale incremental learning,” in *IEEE Conf. Comput. Vis. Pattern Recognit.*, 2019, pp. 374–382.
- [11] F. Zhu, X.-Y. Zhang, C. Wang, F. Yin, and C.-L. Liu, “Prototype augmentation and self-supervision for incremental learning,” in *IEEE Conf. Comput. Vis. Pattern Recognit.*, 2021, pp. 5871–5880.
- [12] Y. Shi, K. Zhou, J. Liang, Z. Jiang, J. Feng, P. H. Torr, S. Bai, and V. Y. Tan, “Mimicking the oracle: an initial phase decorrelation approach for class incremental learning,” in *IEEE Conf. Comput. Vis. Pattern Recognit.*, 2022, pp. 16 722–16 731.
- [13] Z. Zhang, Y. Li, Z. Zhang, C. Jin, and M. Gao, “Adaptive matrix sketching and clustering for semisupervised incremental learning,” *IEEE Signal Process. Lett.*, vol. 25, no. 7, pp. 1069–1073, 2018.
- [14] H. Zhang, B.-B. Gao, Y. Zeng, X. Tian, X. Tan, Z. Zhang, Y. Qu, J. Liu, and Y. Xie, “Learning task-aware language-image representation for class-incremental object detection,” in *Proceedings of the AAAI Conference on Artificial Intelligence*, vol. 38, no. 7, 2024, pp. 7096–7104.
- [15] I. J. Goodfellow, M. Mirza, D. Xiao *et al.*, “An empirical investigation of catastrophic forgetting in gradient-based neural networks,” *arXiv preprint arXiv:1312.6211*, 2013.
- [16] J. Zhu, G. Luo, B. Duan, and Y. Zhu, “Class incremental learning with deep contrastive learning and attention distillation,” *IEEE Signal Process. Lett.*, 2024.
- [17] Y. Liu, B. Schiele, A. Vedaldi *et al.*, “Continual detection transformer for incremental object detection,” in *IEEE Conf. Comput. Vis. Pattern Recognit.*, 2023, pp. 23 799–23 808.
- [18] A. Gupta, S. Narayan, K. Joseph *et al.*, “Ow-detr: Open-world detection transformer,” in *IEEE Conf. Comput. Vis. Pattern Recognit.*, 2022, pp. 9235–9244.
- [19] T. Feng, M. Wang, and H. Yuan, “Overcoming catastrophic forgetting in incremental object detection via elastic response distillation,” in *IEEE Conf. Comput. Vis. Pattern Recognit.*, 2022, pp. 9427–9436.
- [20] D. Zhou, F. Wang, H. Ye *et al.*, “Forward compatible few-shot class-incremental learning,” in *IEEE Conf. Comput. Vis. Pattern Recognit.*, 2022, pp. 9046–9056.
- [21] A. Radford, J. Kim, C. Hallacy *et al.*, “Learning transferable visual models from natural language supervision,” in *Proc. Int. Conf. Mach. Learn.* PMLR, 2021, pp. 8748–8763.
- [22] C. Peng, K. Zhao, and B. Lovell, “Faster ilod: Incremental learning for object detectors based on faster rcnn,” *Pattern Recognit. Lett.*, vol. 140, pp. 109–115, 2020.
- [23] K. Joseph, S. Khan, F. Khan *et al.*, “Towards open world object detection,” in *IEEE Conf. Comput. Vis. Pattern Recognit.*, 2021, pp. 5830–5840.
- [24] X. Gu, T. Lin, W. Kuo *et al.*, “Open-vocabulary object detection via vision and language knowledge distillation,” in *Proc. Int. Conf. Learn. Represent.*, 2022.
- [25] M. Everingham, L. Van G., C. Williams *et al.*, “The pascal visual object classes (voc) challenge,” *International journal of computer vision*, vol. 88, pp. 303–308, 2009.
- [26] K. He, X. Zhang, S. Ren *et al.*, “Deep residual learning for image recognition,” in *IEEE Conf. Comput. Vis. Pattern Recognit.*, 2016, pp. 770–778.
- [27] T. Lin, M. Maire, S. Belongie *et al.*, “Microsoft coco: Common objects in context,” in *Eur. Conf. Comput. Vis.* Springer, 2014, pp. 740–755.